Reduction of Reactive Oxygen Species Ameliorates Metabolism-Secretion Coupling in Islets of Diabetic GK Rats by Suppressing Lactate Overproduction

Mayumi Sasaki,[1] Shimpei Fujimoto,[1,2] Yuichi Sato,[1] Yuichi Nishi,[1,2] Eri Mukai,[1] Gen Yamano,[1] Hiroki Sato,[1] Yumiko Tahara,[1] Kasane Ogura,[1] Kazuaki Nagashima,[1] and Nobuya Inagaki[1]

We previously demonstrated that impaired glucose-induced insulin secretion (IS) and ATP elevation in islets of Goto-Kakizaki (GK) rats, a nonobese model of diabetes, were significantly restored by 30–60-min suppression of endogenous reactive oxygen species (ROS) overproduction. In this study, we investigated the effect of a longer (12 h) suppression of ROS on metabolism-secretion coupling in β-cells by exposure to tempol, a superoxide (O_2^-) dismutase mimic, plus ebselen, a glutathione peroxidase mimic (TE treatment). In GK islets, both H_2O_2 and O_2^- were sufficiently reduced and glucose-induced IS and ATP elevation were improved by TE treatment. Glucose oxidation, an indicator of Krebs cycle velocity, also was improved by TE treatment at high glucose, whereas glucokinase activity, which determines glycolytic velocity, was not affected. Lactate production was markedly increased in GK islets, and TE treatment reduced lactate production and protein expression of lactate dehydrogenase and hypoxia-inducible factor 1α (HIF1α). These results indicate that the Warburg-like effect, which is characteristic of aerobic metabolism in cancer cells by which lactate is overproduced with reduced linking to mitochondria metabolism, plays an important role in impaired metabolism-secretion coupling in diabetic β-cells and suggest that ROS reduction can improve mitochondrial metabolism by suppressing lactate overproduction through the inhibition of HIF1α stabilization. ***Diabetes*** **62:1996–2003, 2013**

In pancreatic β-cells, intracellular glucose metabolism regulates the exocytosis of insulin granules according to metabolism-secretion coupling in which ATP production in mitochondria plays an essential role (1). The reduction of mitochondrial ATP production causes the impairment of glucose-induced IS in various conditions (2).

Reactive oxygen species (ROS) such as superoxide (O_2^-) and hydrogen peroxide (H_2O_2) are normal byproducts of glucose metabolism, including glycolysis and mitochondrial oxidative phosphorylation (3). In pancreatic β-cells, ROS production via nonmitochondrial and mitochondrial pathways has been proposed. In the mitochondrial pathway, ROS is generated in the electron transport chain associated with the mitochondrial membrane potential (4). However, in pathophysiological conditions, NADPH oxidase, an important nonmitochondrial ROS source, may play an important role in ROS generation in β-cells (5). Antioxidant capacity in β-cells is very low because of weak expression of antioxidant enzymes such as catalase, glutathione peroxidase (GPx), and O_2^- dismutase (SOD) in pancreatic islets compared with that in various other tissues (6,7), which suggests vulnerability of β-cells to ROS. Gene expression profiling in islets revealed that SOD, which metabolizes O_2^- to H_2O_2, was 30–40% and GPx, which metabolizes H_2O_2 to H_2O, was 15% of that in liver. Moreover, catalase was not detectable in islets (7).

In β-cells, ROS is one of the most important factors that impair metabolism-secretion coupling (1). Exposure to exogenous H_2O_2, the most abundant ROS, reduces glucose-induced IS by impairing mitochondrial metabolism in β-cells (8). We have proposed that endogenous overproduction of ROS that involves the activation of Src, a nonreceptor tyrosine kinase, plays an important role in impaired metabolism-secretion coupling in islets of diabetic Goto-Kakizaki (GK) rats (9–11). The suppression of the overproduction of ROS for 30–60 min by exposure to ROS scavengers and by suppression of Src activity restores impaired glucose-induced IS and ATP elevation in GK rat islets (9,10). However, the effect of reducing the overproduction of ROS for a longer duration on impaired metabolism-secretion coupling in diabetic β-cells remains unknown.

In the current study, we investigated the effects of 12-h suppression of endogenous ROS production on impaired metabolism-secretion coupling in β-cells by exposing cell-permeable antioxidant enzyme mimics, including tempol, an SOD mimic (12), and ebselen, a GPx mimic (13), which are commonly used in the field of diabetology without cytotoxic effects (14,15). Our results indicate that 12-h suppression of ROS improves metabolism-secretion coupling by a mechanism different from that involved in improvement by ROS reduction for 30–60 min.

RESEARCH DESIGN AND METHODS

Materials. Ebselen was purchased from Calbiochem (La Jolla, CA). HEPES, KCl, EGTA, glucose, NaCl, $NaHCO_3$, $HClO_4$, Na_2CO_3, H_2O_2, BSA, and the substrates used in ATP production, except glycerol phosphate, were purchased from Nacalai (Kyoto, Japan). [U-^{14}C]-glucose was obtained from GE Healthcare (Uppsala, Sweden). Lactate dehydrogenase (EC 1.1.1.27) and Dowex 1 × 8 anion exchange resin (formate) (50–100 mesh) were obtained from Wako (Osaka, Japan). Hypoxia-inducible factor 1α (HIF1α) inhibitor (3-[2-(4-adamantan-1-yl-phenoxy)-acetylamino]-4-hydroxybenzoic acid methyl ester) was obtained from Merck Millipore (Darmstadt, Germany). All other reagents were obtained from Sigma-Aldrich (St. Louis, MO).

Animals. Male Wistar and GK rats were obtained from Shimizu (Kyoto, Japan). All experiments were carried out with rats 7–10 weeks of age. The body weight

From the [1]Department of Diabetes and Clinical Nutrition, Graduate School of Medicine, Kyoto University, Kyoto, Japan; and the [2]Department of Endocrinology, Metabolism, and Nephrology, Kochi Medical School, Kochi University, Nankoku, Japan.
Corresponding author: Nobuya Inagaki, inagaki@metab.kuhp.kyoto-u.ac.jp.
Received 6 July 2012 and accepted 22 December 2012.
DOI: 10.2337/db12-0903
This article contains Supplementary Data online at http://diabetes.diabetesjournals.org/lookup/suppl/doi:10.2337/db12-0903/-/DC1.

See accompanying commentary, p. 1823.

of GK rats used in the experiments was similar to that of Wistar rats (means ± SE; Wistar, 231 ± 3, vs. GK, 217 ± 3 g, not significant). The nonfasting plasma glucose of GK rats was higher compared with that of Wistar rats (means ± SE; Wistar, 5.72 ± 0.12, vs. GK, 11.57 ± 0.58 mmol/L, $P < 0.01$). The animals were maintained and used in accordance with the guidelines of the animal care committee of Kyoto University.

Islet isolation and culture. Pancreatic islets were isolated from Wistar and GK rats by collagenase digestion as described previously (16). Isolated islets were washed with Krebs-Ringer bicarbonate buffer (KRBB) containing 2.8 mmol/L glucose and cultured for 12 h in RPMI-1640 medium containing 10% FCS and 5.5 mmol/L glucose without or with 10 mmol/L tempol, 10 μmol/L ebselen, or combination of tempol and ebselen (TE treatment) at 37°C in humidified air containing 5% CO_2. Insulin content of GK islets was similar to that of Wistar islets (means ± SE; Wistar, 20.0 ± 2.2, vs. GK, 23.0 ± 2.6 ng/islet, not significant).

Measurement of O_2^- and H_2O_2 generations. O_2^- and the H_2O_2 production were measured at the end of the 12-h culture in conditions described above. O_2^- generation was detected by nitroblue tetrazolium (NBT) assay (17) using KRBB supplemented with 0.2% BSA (fraction V) and 10 mmol/L HEPES adjusted to pH 7.4 (KRBB medium). Groups of 100 islets were batch incubated in tubes containing 0.5 mL KRBB medium supplemented with 5.5 mmol/L glucose with 0.2% (weight/volume) NBT at 37°C for 30 min. After the islets were centrifuged (1,000 rpm for 2 min at 4°C), the supernatant was removed and formazan-NBT (NBT reduced) was dissolved in 100 μL 50% (volume/volume) acetic acid by sonication (5-s pulse, five times). The sonicate was briefly centrifuged, and the absorbance of the supernatant was measured at 560 nm using a spectrofluorometer (Shimadzu RF-5000, Kyoto, Japan). H_2O_2 release from islets was measured according to the method previously described (18). In brief, islets were cultured for 12 h in various conditions as described above. Groups of 150 islets were batch incubated for 60 min in KRBB medium containing 5.5 mmol/L glucose with 0.1 mg/mL horseradish peroxidase (type II) and 0.44 mmol/L homovanillic acid. After the islets were centrifuged (1,000 rpm for 2 min at 4°C), the supernatant was removed. Fluorescence of the supernatant was measured at excitation and emission of 315 and 425 nm, respectively, using a spectrofluorometer (Shimadzu RF-5000). Standard curves were produced using samples containing known amounts of H_2O_2 without islets.

Measurement of insulin release, ATP contents, and glucose oxidation. Insulin release from islets was monitored using batch incubation as described previously (16). ATP content in islets was determined as previously described (9). ATP contents were measured using ENLITEN luciferin-luciferase solution (Promega, Madison, WI) by luminometer (GloMax 20/20n; Promega). Glucose oxidation was carried out using the previously described method (19).

Intraperitoneal glucose tolerance tests. After GK rats were divided into two groups, one group received intraperitoneal injection of tempol (50 mg/kg) and ebselen (10 mg/kg) twice (12 and 6 h before intraperitoneal glucose tolerance tests [ip-GTTs]) during a 15-h fast (TE); the other group was treated similarly with vehicle alone. After these treatments, ip-GTTs (1 g/kg body weight) were performed. Plasma glucose and plasma insulin levels were measured in samples taken at the indicated times. Plasma glucose levels were determined by the glucose oxidase method. Plasma insulin levels were determined using an enzyme immunoassay (Shibayagi, Gunma, Japan).

Immunoblot analysis. The preparations for whole-islet lysate and for the mitochondrial fraction were described previously (20,21). Western blotting was performed as previously described (20) with the following antibodies: mouse monoclonal anti–complex I (39 kDa subunit), anti–complex III (core II),

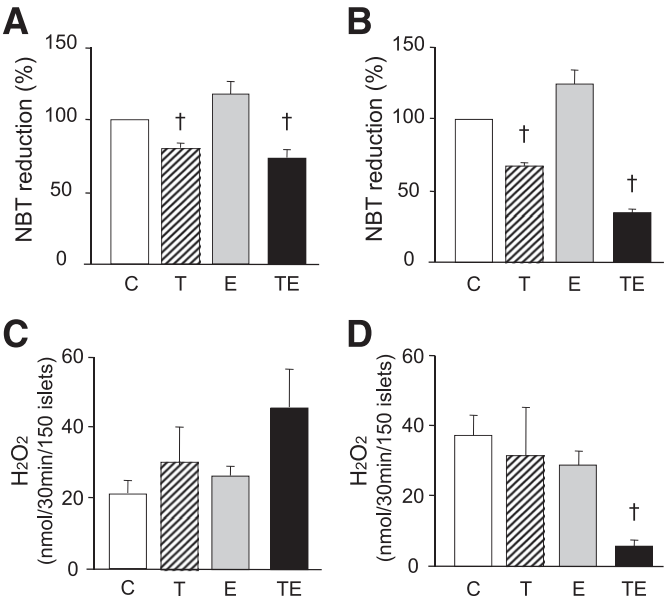

FIG. 1. Effects of antioxidant enzyme mimics on ROS production in Wistar (*A* and *C*) and GK (*B* and *D*) islets. Islets were isolated and cultured without (control [C]; white bars) or with 10 mmol/L tempol (T; hatched bars), 10 μmol/L ebselen (E; gray bars), or T plus E (TE; black bars). O_2^- generation (*A* and *B*) was determined by measuring the reduction of NBT using 100 islets, and data were shown as fold increase relative to control. H_2O_2 generation (*C* and *D*) was determined by measuring the peroxidation of homovanillic acid included in the reaction mixtures as a substrate using 150 islets. Data are shown as means ± SE of three different experiments. †$P < 0.01$ vs. control.

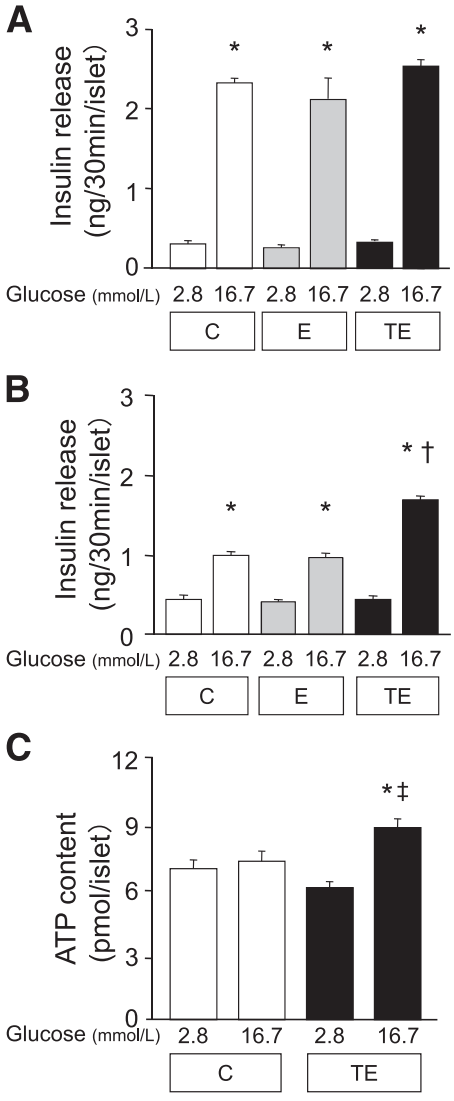

FIG. 2. Effects of antioxidant enzyme mimics on IS (*A* and *B*) and ATP contents (*C*). Islets were cultured without (control [C]) or with ebselen (E; gray bars) and tempol plus ebselen (TE; black bars) for 12 h. After cultured islets were washed and preincubated with 2.8 mmol/L glucose for 30 min, islets were incubated for 30 min at 2.8 and 16.7 mmol/L glucose, and released insulin was measured. Insulin release from Wistar islets (*A*) and in GK islets (*B*) is shown. After cultured GK islets were washed and preincubated with 2.8 mmol/L glucose for 30 min, islets were incubated for 30 min at 2.8 and 16.7 mmol/L glucose, and ATP contents in GK islets were measured (*C*). Data are expressed as the mean ± SE of 25 (*A* and *B*) or 20 (*C*) determinations from three (*A* and *C*) and four (*B*) experiments. *$P < 0.01$ vs. corresponding 2.8 mmol/L glucose; †$P < 0.01$ vs. 16.7 mmol/L glucose in control; ‡$P < 0.05$ vs. 16.7 mmol/L glucose in control.

anti–complex IV (subunit I), and anti–complex V (subunit α) of the mitochondrial respiratory chain (1:1,000) from Invitrogen (Carlsbad, CA), mouse anti–β-actin (1:5,000) from Sigma-Aldrich, rabbit polyclonal anti–LDH-A (1:1,000) from Cell Signaling (Danvers, MA), rabbit anti–PDK-1 (1:1,000) and rabbit anti-HIF1α (1:250) from Abcam (Paris, France), rabbit anti-UCP2 (1:200) from Chemicom (Temecula, CA), mouse anti–hsp-60 (1:5,000) from BD Biosciences (Franklin Lakes, NJ), rabbit anti–PK-M2 (1:2,500) from Novus Biological, LLC (Littleton, CO), and horseradish peroxidase–conjugated anti-rabbit and -mouse antibody (1:5,000) from GE Healthcare. Proteins were detected using an enhanced chemiluminescence system (GE Healthcare). Protein density was quantified by densitometric analysis using Multi Gauge software (Fujifilm, Tokyo, Japan).

Measurements of enzyme activities. After islets were cultured with or without TE for 12 h, whole-islet homogenates and mitochondrial fractions from cultured islets were obtained. Glucokinase and hexokinase activities were determined using whole-islet homogenates by NADH formation in an enzyme reaction as previously described (22). The activity of mitochondrial glycerol phosphate dehydrogenase (mGPDH) in whole-islet homogenates of Wistar and GK rats was measured by the reduction of 2-*p*-iodo-3-*p*-nitro-5-phenyltetrezolium to indoformazan as previously described (23). The activity of mGPDH in the mitochondrial fraction from GK islets was measured by the method based on the generation of ^{3}HOH from L-[2-^{3}H]glycerol-3-phosphate (24). In brief, after mitochondrial fractions were incubated at 37°C for 30 min with 2.5 mCi/mmol L-[2-^{3}H] glycerol-3-phosphate and the reaction was stopped by the addition of antimycin A, the mixture was immediately applied to a column of Dowex 1-X8 (formate), which was washed with 0.5 mL water. The radioactivity of the column effluent was measured by a liquid scintillation counter.

Measurement of mitochondrial ATP production. The mitochondrial fraction from islets and measurement of ATP production were performed as previously described (21).

Measurement of lactate production. Lactate production was measured as previously described (25). In brief, after preincubation, groups of 20 islets were batch incubated in KRBB medium containing 2.8 and 16.7 mmol/L glucose for 60 min at 37°C. The supernatant (200 μL) was mixed with 0.5 mL of 0.5 mol/L glycine/0.4 mol/L hydrazine buffer (pH 9.0) containing 2.4 mmol/L NAD and 7.2 units/mL lactate dehydrogenase, and was incubated for 30 min at 37°C. The fluorescence of NADH was then measured at an excitation of 340 nm and emission of 450 nm. Standard curves were produced from samples containing known amounts of lactate.

Statistical analysis. The data are expressed as means ± SE. Statistical significance was determined by unpaired Student *t* test. $P < 0.05$ was considered significant.

RESULTS

O_2^- and H_2O_2 production during culture with antioxidant mimics. Tempol, an SOD mimic, decreased O_2^- production in Wistar (Fig. 1*A*) and GK islets (Fig. 1*B*) but had no effect on H_2O_2 production in either of the islets (Fig. 1*C* and *D*). Ebselen, a GPx mimic, had no reducing effect on O_2^- and H_2O_2 production in either of the islets (Fig. 1). Cotreatment with TE reduced O_2^- production by 27.0% but had no effect on H_2O_2 production in Wistar islets (Fig. 1*A* and *C*). On the other hand, in GK islets, TE treatment prominently reduced O_2^- and H_2O_2 production by 65.0 and 84.6%, respectively (Fig. 1*B* and *D*). Taken together, these findings indicate that TE treatment is effective in reducing oxidative stress in GK islets.

Effect of TE treatment on IS. The effect of antioxidant mimics on β-cell function was investigated. In the presence of 16.7 mmol/L glucose, insulin secretion (IS) from GK islets was reduced compared with that from control Wistar rats (GK, 1.01 ± 0.06, vs. Wistar, 2.32 ± 0.11 ng/30 min/islet, $P < 0.01$). Although TE treatment had no effect on IS from Wistar islets (Fig. 2*A*), it restored high glucose–induced IS (Fig. 2*B*) and ATP content (Fig. 2*C*) in GK islets. We demonstrated previously that impaired glucose-induced IS in GK islets was significantly restored by acute exposure to PP2, a Src inhibitor (9). To examine the involvement of Src inhibition in the improvement of glucose-induced IS after TE treatment, TE-treated GK islets were incubated for 30 min with or without 10 μmol/L PP2 in the presence of 16.7 mmol/L glucose. In TE-treated GK islets, 30-min exposure to PP2 prominently enhanced IS at high glucose (control, 1.71 ± 0.07, vs. PP2, 4.06 ± 0.22 ng/30 min/islet, $P < 0.01$), which implies involvement of an independent mechanism of Src inhibition in the improvement of glucose-induced IS by chronic TE treatment.

To investigate the effects of TE treatment on β-cell function in vivo, a GTT was assessed after intraperitoneal TE administration (Table 1). In GK rats, TE treatment decreased the glucose level at 15 and 30 min and increased insulin levels at 30 min after glucose loading. Studies using isolated islets from GK rats after TE treatment in vivo revealed that high glucose–induced IS was increased by TE treatment (Table 2).

Effect of TE treatment on expression of UCP2 and mitochondrial respiratory chain proteins. Immunoblot analysis showed that TE treatment had no effect on protein levels of UCP2 in protein extracts of the islet mitochondrial fraction (Supplementary Fig. 1*A*) and on those of complex I, III, IV, and V of the mitochondrial respiratory chain in lysates of whole islets (Supplementary Fig. 1*B*) in both GK and Wistar islets.

Effect of TE treatment on glucose metabolism. TE treatment had no effect on glucokinase and hexokinase activities, which determines the velocity of glycolysis in β-cells (26), in GK and Wistar islets (Table 3). By TE treatment, glucose oxidation at high glucose, an indicator of Krebs cycle velocity, was not affected in Wistar islets, whereas it was significantly increased in GK islets (control, 25.4 ± 4.1, vs. TE, 55.8 ± 12.2 pmol/islet/90 min, $P < 0.05$) (Fig. 3).

Effect of TE treatment on ATP production and on activity of mGPDH. ATP production by mitochondria from control and TE-treated islets of Wistar and GK rats was measured in the presence of various substrates and inhibitors (Table 4), including succinate (electron transfer at complex I by NADH generation in the Krebs cycle and at complex II directly), succinate with rotenone (electron

TABLE 1
Ip-GTT in GK rats treated with TE in vivo

		Minute				
		0	15	30	60	120
Glucose (mg/dL)	Control	145 ± 4	475 ± 6	423 ± 11	340 ± 14	184 ± 7
	TE	144 ± 11	330 ± 41†	359 ± 28*	330 ± 24	200 ± 13
Insulin (pg/mL)	Control	164 ± 70	ND	172 ± 50	ND	205 ± 75
	TE	205 ± 32	ND	400 ± 101*	ND	209 ± 46

After the intraperitoneal injection of 50 mg/kg tempol plus 10 mg/kg ebselen (TE) or vehicle alone (control) twice during a 15-h fast in GK rats, GTT with intraperitoneal injection of glucose (1 g/kg body weight) was performed and plasma glucose and insulin levels were measured. Data are means ± SE of seven independent experiments. ND, not determined. *$P < 0.05$ vs. corresponding control TE. †$P < 0.01$ vs. corresponding control without TE.

TABLE 2
Insulin secretion from isolated islets in GK rats treated with tempol plus ebselen in vivo

	2.8 mmol/L glucose	16.7 mmol/L glucose
Control (ng/30 min/islet)	0.40 ± 0.04	0.84 ± 0.06
TE (ng/30 min/islet)	0.49 ± 0.04	1.42 ± 0.13*

After the intraperitoneal injection of 50 mg/kg tempol plus 10 mg/kg ebselen (TE) or vehicle alone (control) twice during a 15-h fast in GK rats, islets were isolated and IS in the presence of 2.8 and 16.7 mmol/L glucose was measured. Data are means ± SE of nine determinations. *$P < 0.01$ vs. corresponding control without TE.

transfer at complex II and inhibition of electron transfer through NADH at complex I), glutamate plus malate (electron transfer mainly at complex I by NADH generation derived from reaction via glutamate dehydrogenase), pyruvate plus malate (electron transfer mainly at complex I by NADH generation derived from reaction via pyruvate dehydrogenase), ascorbate plus N,N,N′,N′-tetramethyl-p-phenylenediamine (TMPD) (electron transfer at complex IV directly), and glycerol-3-phosphate (G3P) (electron transfer at complex II by $FADH_2$ generation derived from reaction via mGPDH). Control and TE-treated mitochondria showed similar rates of ATP production for all substrates tested, except for G3P. TE treatment promotes the rate of mitochondrial ATP production in the presence of G3P in Wistar and GK islets 3.3- and 2.2-fold, respectively. In the measurement of activity of mGPDH using whole islet homogenates, the value in GK islets was lower compared with that of Wistar islets, and enhancement of the activity by TE treatment was not significant in either Wistar or GK islets (Table 3). However, in the measurement of activity of mGPDH using intact mitochondria, TE treatment increased mGPDH activity in GK mitochondria (Table 3).

Lactate production and protein expression of lactate dehydrogenase and HIF1α. Lactate production in GK islets was significantly higher compared with that in Wistar islets at both basal and stimulated levels of glucose (at 2.8 mmol/L glucose: Wistar, 1.32 ± 0.15, vs. GK, 8.15 ± 1.36, $P < 0.01$; at 16.7 mmol/L glucose: Wistar, 3.09 ± 0.33, vs. GK, 14.08 ± 1.68, $P < 0.01$) (Fig. 4*A*). TE treatment suppressed lactate production at both basal and stimulated levels of glucose in both Wistar and GK islets; the most prominent reduction in these conditions was at 16.7 mmol/L glucose in GK islets (control, 14.08 ± 1.68, vs. TE, 5.71 ± 0.79, $P < 0.01$). Protein expression levels of HIF1α, a potential upstream regulator of lactate dehydrogenase (LDH), in INS-1 cells were gradually increased over 12 h in the presence of 200 μmol/L $CoCl_2$, a chemical inducer of HIF1α (27) (Supplementary Fig. 2). TE treatment time-dependently suppressed HIF1α levels in GK islets, and the reduction was significant after 9-h TE treatment (~30% reduction at 9 h; ~50% reduction at 12 h) (Fig. 4*B*). Protein expression levels of HIF1α and HIF1α downstream targets, including LDH-A and pyruvate dehydrogenase-1 (PDK-1), were examined 12 h after TE treatment. In GK islets, TE treatment significantly decreased HIF1α, LDH-A, and M2-PK expression (HIF1α, ~50% reduction; LDH-A, ~30% reduction; M2-PK, ~30% reduction) but did not affect PDK-1 expression (Fig. 4*C* and Supplementary Fig. 3).

Effect of HIF1α inhibitor on IS and lactate production in GK islets. IS in the presence of 16.7 mmol/L glucose from GK islets was enhanced by HIF1α inhibitor treatment (control, 1.34 ± 0.07, vs. HIF1α inhibitor, 1.77 ± 0.09 ng/30 min/islet, $P < 0.01$). Lactate production in the presence of 2.8 and 16.7 mmol/L glucose was reduced by HIF1α inhibitor treatment (2.8 mmol/L glucose: control, 12.44 ± 1.12, vs. HIF1α inhibitor, 9.46 ± 0.89 pmol/islet, $P < 0.01$; 16.7 mmol/L glucose: control, 15.39 ± 1.02, vs. HIF1α inhibitor, 12.42 ± 1.40 pmol/islet, $P < 0.01$) (Fig. 5).

DISCUSSION

The current study demonstrates that combination treatment by tempol, an SOD mimic, and ebselen, a GPx mimic (TE treatment), efficiently suppressed both H_2O_2 and O_2^- production in GK islets. Moreover, impaired glucose-induced IS and ATP elevation in GK islets were significantly improved by TE treatment but were not improved by tempol or ebselen alone. These results are compatible with previous studies in which coexpression of the antioxidant enzymes in a β-cell line was more efficient than expression of either single enzyme in reducing ROS production and oxidative injury (7,28,29).

We then examined the precise mechanisms of the improvement in glucose-induced ATP elevation in GK islets by TE treatment. UCP2 decreases mitochondrial ATP production by reducing mitochondrial hyperpolarization derived from an increase in mitochondrial proton conductance. UCP2 negatively regulates metabolism-secretion

TABLE 3
Effect of TE treatment on glucokinase, hexokinase, and mitochondrial G3P dehydrogenase activities

Experimental conditions		Wistar rat	GK rat
Hexokinase (whole islet extracts)	Control	21.58 ± 3.23	131.46 ± 23.62
(pmol/islet/h)	TE	21.63 ± 3.18	138.19 ± 35.97
Glucokinase (whole islet extracts)	Control	22.79 ± 8.21	52.71 ± 8.82
(pmol/islet/h)	TE	22.90 ± 6.53	42.41 ± 8.96
mGPDH (whole islet extracts)	Control	9.90 ± 0.34	6.76 ± 0.32*
(nmol/mg protein/min)	TE	10.60 ± 0.75	7.37 ± 0.14
mGPDH (mitochondrial fraction)	Control	ND	65.77 ± 1.61
(nmol/mg mitochondrial protein/min)	TE	ND	75.41 ± 2.34†

After islets were cultured with or without TE for 12 h, extract from whole islets and mitochondrial fractions were obtained. Data are given as the mean ± SE from five experiments for glucokinase and hexokinase, six experiments for mGPDH using whole-islet extracts, and three experiments for mGPDH using the mitochondrial fraction. ND, not determined. *$P < 0.05$ vs. Wistar control without TE. †$P < 0.05$ vs. control without TE.

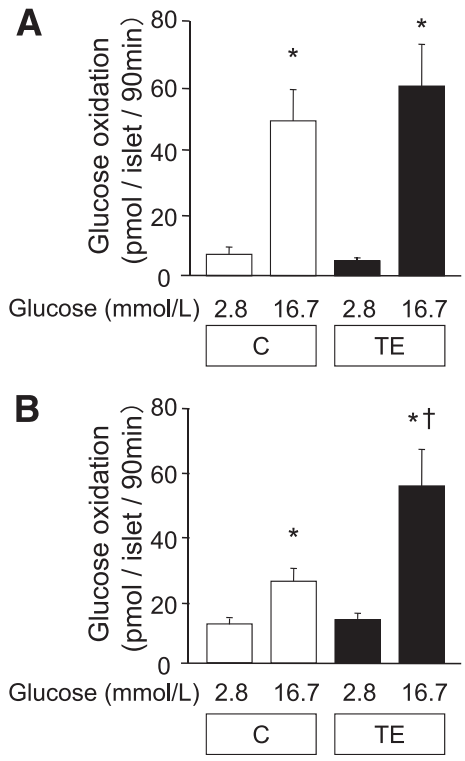

FIG. 3. Effects of TE treatment on glucose oxidation in Wistar (*A*) and GK (*B*) islets. Islets were cultured without (control [C]; open bars) or with TE (black bars) for 12 h. After cultured islets were preincubated with 2.8 mmol/L glucose for 30 min, glucose oxidation during incubation for 90 min in the presence of 2.8 and 16.7 mmol/L glucose was measured in islets. Data are shown as means ± SE of 12 determinations from three (A) and four (B) experiments. *$P < 0.01$ vs. corresponding 2.8 mmol/L glucose; †$P < 0.01$ vs. 16.7 mmol/L glucose in control.

coupling in β-cells (30,31). However, regulation of UCP2 expression may not play an important role in the mechanism, as the UCP2 expression level was not affected in GK islets by TE treatment. Western blot analysis revealed that the expression of respiratory chain proteins, including complex I, III, IV, and V, was not affected by TE treatment. In addition, the relative mRNA levels of nuclear factors, including *NRF-1*, *NRF-2*, and *TFAM*, which affect mitochondrial biogenesis, also were not altered by TE treatment (data not shown). These results indicate that the regulation of mitochondrial mass is not involved in the mechanism.

ATP production is driven by the H^+ gradient across the mitochondrial membrane generated by the transport of high-energy electrons in the respiratory chain. These electrons are derived from NADH and $FADH_2$, derived from the Krebs cycle in the matrix and/or transferred from the cytosol by the shuttle system. To determine which step in mitochondrial carbohydrate metabolism is affected in TE-treated islets, ATP production in the presence of various substrates and inhibitors was measured using mitochondrial fractions from the cultured islets. In the presence of G3P, ATP production was increased by TE treatment in both the Wistar and GK mitochondrial fraction. Transfer of a reduced equivalent from cytosol to mitochondria by the glycerol phosphate shuttle may well play a more important role in mitochondrial ATP production in islets than in other tissues, since the activity of mGPDH, a key enzyme in the glycerol phosphate shuttle is ~60-fold higher in islets than in other tissues (24). In addition, decreased activity is observed in diabetic islets (32). Although an increase in the activity of mGPDH by TE treatment was detected, the increase was similar in the mitochondrial fraction from both GK and Wistar islets. Therefore, an improvement of mGPDH activity alone may not account for the improvement in glucose-induced ATP elevation in GK islets by TE treatment.

TE treatment did not affect the activity of glucokinase, a rate-limiting enzyme in glycolysis (26). In contrast, glucose oxidation at high glucose, which reflects Krebs cycle velocity, was improved in GK islets by TE treatment. These results suggest that coupling between glycolysis and mitochondrial oxidation, which plays an important role in glucose-induced IS (33), is improved by TE treatment. Lactate production weakens coupling between glycolysis and mitochondrial oxidation by decreasing the pyruvate supply to mitochondria. In several studies, the overexpression of LDH-A in β-cells attenuated glucose-induced IS (34–36) with an increase in lactate production (34,37). In addition, lactate release from β-cells increases in parallel with a decrease in the glucose oxidation rate (36). These findings support the hypothesis that regulation of lactate production may play an important role in the improvement of metabolism-secretion coupling by TE treatment. In the current study, lactate production in GK islets was higher compared with that in control, as shown in a previous study (38), and it was reduced by TE treatment. The protein expression level of LDH-A, an enzyme that catalyzes the reaction from pyruvate and NADH to lactate and NAD^+, was 8.6-fold higher in GK islets compared with

TABLE 4
ATP production by mitochondria fraction from islets

Experimental conditions	Wistar rat		GK rat	
	C	TE	C	TE
0.5 mmol/L succinate	2.86 ± 0.42	2.58 ± 0.15	2.43 ± 0.27	2.18 ± 0.21
0.5 mmol/L succinate + 1 μmol/L antimycin A	0.40 ± 0.03	0.46 ± 0.02	0.36 ± 0.00	0.36 ± 0.00
1 mmol/L succinate + 1 μmol/L rotenone	3.96 ± 0.48	3.55 ± 0.26	2.92 ± 0.22	2.71 ± 0.48
1 mmol/L glutamate + 1 mmol/L malate	0.92 ± 0.23	0.86 ± 0.14	0.87 ± 0.13	0.90 ± 0.14
1 mmol/L pyruvate + 1 mmol/L malate	1.32 ± 0.38	1.17 ± 0.29	1.27 ± 0.22	1.23 ± 0.22
0.5 mmol/L TMPD + 2 mmol/L ascorbate	5.42 ± 0.41	4.91 ± 0.15	6.27 ± 0.62	5.94 ± 0.54
1 mmol/L G3P	0.92 ± 0.14	3.03 ± 0.17†	0.69 ± 0.05	1.50 ± 0.12†

Islets were cultured with or without TE for 12 h. Mitochondrial suspension was obtained from control (C) or TE-treated islets (TE). Mitochondrial ATP production is indicated as the ratio to ATP production from adenylate kinase to normalize the mass of the intact mitochondria obtained, which was determined from the same sample in parallel incubation. Data are given as the mean ± SE of three different experiments. †$P < 0.01$ vs. control without TE.

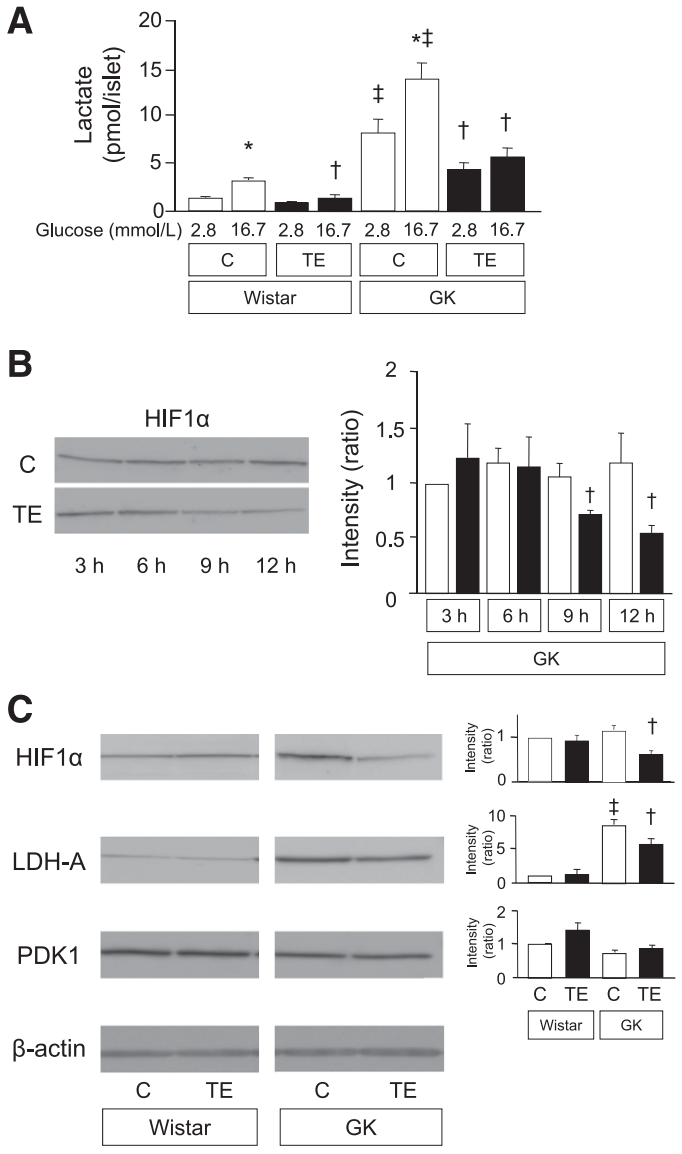

FIG. 4. Effects of TE treatment on lactate production and HIF1α signaling. Islets were cultured without (control [C]; open bars) or with TE (black bars) for 12 h. *A*: Effects of TE treatment on lactate production in Wistar and GK islets. After cultured islets were preincubated under 2.8 mmol/L glucose for 30 min, 20 islets were batch incubated in the medium containing 2.8 and 16.7 mmol/L glucose for 60 min at 37°C, and released lactate in the medium was measured. Values are means ± SE of 13 determinations from three (Wistar) and four (GK) experiments. *B*: Time course of HIF1α protein levels in GK and Wistar islets during TE treatment using whole-islet lysates. Islets were cultured without (C; open bars) or with TE (closed bars) for indicated hours. The bar graphs are expressed relative to 3 h–cultured control values corrected by β-actin level. The values are means ± SE of determinations from three different experiments. Representative blot panels are shown. *C*: Effect of TE treatment on protein levels of HIF1α and HIF1α downstream target proteins in whole lysate of Wistar and GK islets. Representative blot (*left*) and quantification data (*right*) are shown. The bar graphs are expressed relative to Wistar without TE treatment values corrected by β-actin level. The values are means ± SE of determinations from three different experiments. *$P < 0.01$ vs. corresponding 2.8 mmol/L glucose; †$P < 0.01$ vs. corresponding control without TE; ‡$P < 0.01$ vs. corresponding Wistar.

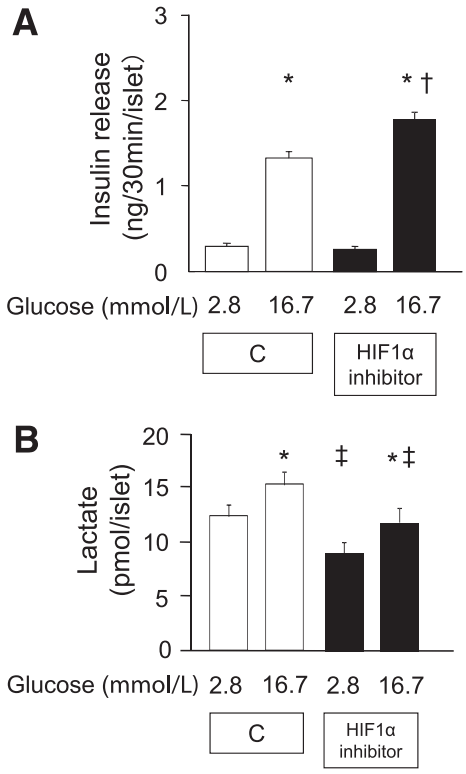

FIG. 5. Effects of HIF1α inhibitor on IS and lactate production in GK islets. Islets were cultured without (control [C]; open bars) or with 1 μmol/L HIF1α inhibitor (black bars) for 12 h. *A*: Insulin secretion. After cultured islets were preincubated with 2.8 mmol/L glucose for 30 min, IS during incubation for 30 min in the presence of 2.8 and 16.7 mmol/L glucose was measured in islets. Data are shown as means ± SE of 25 determinations from three experiments. *$P < 0.01$ vs. corresponding 2.8 mmol/L glucose; †$P < 0.01$ vs. 16.7 mmol/L glucose in control. *B*: Lactate production. After cultured islets were preincubated under 2.8 mmol/L glucose for 30 min, islets were batch incubated in the medium containing 2.8 and 16.7 mmol/L glucose for 60 min, and released lactate in the medium was measured. Values are means ± SE of 12 determinations from three experiments. *$P < 0.01$ vs. corresponding 2.8 mmol/L glucose; ‡$P < 0.01$ vs. corresponding control without HIF1α inhibitor.

control Wistar islets, and was reduced by ~30% after TE treatment. In nondiabetic pancreatic β-cells, low LDH activity together with high mGPDH activity may act as a device to transfer NADH in the cytosol to the mitochondria and reduce lactate production by decreasing the NADH level in cytosol (39). In GK islets, enhanced LDH activity and reduced mGPDH activity might produce lactate overproduction and reduce mitochondrial oxidation by decreasing the supply of pyruvate and reducing equivalents to mitochondria and by an increase in the availability of cytosolic NADH to produce lactate from pyruvate as well. In this case, reduced LDH activity and increased mGPDH activity by TE treatment may well have decreased lactate overproduction and ameliorated metabolism-secretion coupling in GK islets.

These metabolic profiles in GK islets resemble the Warburg effect, characteristic aerobic metabolism in cancer cells by which lactate is overproduced from glucose even under nonhypoxic conditions (40). HIF1α is a transcription factor that functions as a master regulator of oxygen homeostasis and upregulates the expression of *LDH* (41). HIF1α activity is controlled at the level of protein stability. When oxygen is present, two proline residues in the oxygen-dependent degradation domain of HIF1α are hydroxylated by the prolylhydroxylase enzymes (PHDs) (42). These hydroxylated motifs allow capture by the von Hippel-Lindau protein that forms the recognition component of an E3 ubiquitin ligase complex, which targets the hydroxylated HIF1α for polyubiquitination and proteasomal degradation (43). In the current study, TE treatment showed a time-dependent decrease in HIF1α protein levels

in GK islets and 50% reduction compared with that in nontreated GK islets at 12-h culture, which could reduce LDH-A protein in TE-treated GK islets. The Warburg effect is usually thought of as a high rate of glycolysis. Since TE treatment did not affect glucokinase activity, which determines glycolytic velocity in β-cells, alteration in the HIF1α level in the pathophysiological range may not affect glycolytic velocity in β-cells. In this respect, lactate overproduction in GK islets differs from the typical Warburg effect.

HIF1α downregulates the expression of GLUT2 and glucokinase and upregulates PDK-1, which inactivates pyruvate dehydrogenase and suppresses metabolism in the Krebs cycle (44) in islets of von Hippel-Lindau gene (*vhl*)-deficient mice (45). On the contrary, TE treatment did not affect the glucokinase activity and protein level of PDK-1 in GK islets. This discrepancy is not fully understood, but one possibility is that the expression level of HIF1α may be higher than the pathophysiological level in *vhl*-deficient islets. This is supported by the fact that glucose-induced IS is impaired severely and almost abolished in *vhl*-deficient islets. The transcript level of *LDH-A* in *vhl*-deficient islets is about 20-fold higher compared with control islets, which is much higher than that of *PDK-1* (~5-fold) (46). This suggests that the expression of LDH-A is more readily affected by HIF1α expression than that of PDK-1.

An increase in the basal HIF1α level in GK islets was not found compared with that in Wistar islets. In contrast, basal levels of LDH-A in GK islets was prominently increased compared with that in Wistar islets, suggesting that regulators other than HIF1α may play an important role in the enhancement of basal LDH-A in GK islets. However, our finding in the current study remains valid, as ROS-dependent regulation of LDH-A by HIF1α, which plays an important role in lactate overproduction and impaired glucose-induced IS in GK islets, was established. In addition, the involvement of HIF1α in lactate overproduction was shown clearly by the finding that HIF1α inhibitor treatment restored high glucose–induced IS and suppressed lactate production in GK islets. ROS inhibits PHD activity and stabilizes HIF1α (47,48). In GK islets, an excess amount of ROS may inhibit PHD activity and stabilize the HIF1α protein. Thus, TE treatment may recover PHD activity by reducing the ROS level and decreasing the HIF1α protein level to eventually ameliorate metabolism-secretion coupling in GK islets.

In conclusion, we show that 12-h suppression of endogenous ROS, including O_2^- and H_2O_2, improves impaired metabolism-secretion coupling in GK islets. Our results suggest that lactate overproduction plays an important role in impaired metabolism-secretion coupling in diabetic β-cells; ROS reduction improves mitochondrial metabolism by suppressing lactate overproduction through the inhibition of HIF1α stabilization.

ACKNOWLEDGMENTS

This study was supported by a Research Grant on Nanotechnical Medicine from the Ministry of Health, Labour and Welfare of Japan; scientific research grants; a grant from the Innovation Cluster Kansai project of the Ministry of Education, Culture, Sports, Science and Technology of Japan; and a grant from CREST of the Japan Science and Technology Cooperation.

No potential conflicts of interest relevant to this article were reported.

M.S. researched data, contributed to the discussion, wrote the manuscript, and reviewed and edited the manuscript. S.F. contributed to the discussion, wrote the manuscript, and reviewed and edited the manuscript. Y.S., Y.N., E.M., G.Y., H.S., Y.T., and K.O. researched data. K.N. and N.I. contributed to the discussion, and reviewed and edited the manuscript. S.F. is the guarantor of this work and, as such, had full access to all the data in the study and takes responsibility for the integrity of the data and the accuracy of the data analysis.

Parts of this study were presented in abstract form at the 72nd Scientific Sessions of the American Diabetes Association, Philadelphia, Pennsylvania, 8–12 June 2012.

The authors thank C. Kotake and M. Akazawa (Kyoto University) for technical assistance.

REFERENCES

1. Fujimoto S, Mukai E, Inagaki N. Role of endogenous ROS production in impaired metabolism-secretion coupling of diabetic pancreatic β cells. Prog Biophys Mol Biol 2011;107:304–310
2. Fujimoto S, Nabe K, Takehiro M, et al. Impaired metabolism-secretion coupling in pancreatic β-cells: role of determinants of mitochondrial ATP production. Diabetes Res Clin Pract 2007;77(Suppl 1):S2–S10
3. Bindokas VP, Kuznetsov A, Sreenan S, Polonsky KS, Roe MW, Philipson LH. Visualizing superoxide production in normal and diabetic rat islets of Langerhans. J Biol Chem 2003;278:9796–9801
4. Turrens JF. Mitochondrial formation of reactive oxygen species. J Physiol 2003;552:335–344
5. Guichard C, Moreau R, Pessayre D, Epperson TK, Krause KH. NOX family NADPH oxidases in liver and in pancreatic islets: a role in the metabolic syndrome and diabetes? Biochem Soc Trans 2008;36:920–929
6. Grankvist K, Marklund SL, Täljedal IB. CuZn-superoxide dismutase, Mn-superoxide dismutase, catalase and glutathione peroxidase in pancreatic islets and other tissues in the mouse. Biochem J 1981;199:393–398
7. Tiedge M, Lortz S, Munday R, Lenzen S. Complementary action of antioxidant enzymes in the protection of bioengineered insulin-producing RINm5F cells against the toxicity of reactive oxygen species. Diabetes 1998;47:1578–1585
8. Maechler P, Jornot L, Wollheim CB. Hydrogen peroxide alters mitochondrial activation and insulin secretion in pancreatic beta cells. J Biol Chem 1999;274:27905–27913
9. Kominato R, Fujimoto S, Mukai E, et al. Src activation generates reactive oxygen species and impairs metabolism-secretion coupling in diabetic Goto-Kakizaki and ouabain-treated rat pancreatic islets. Diabetologia 2008;51:1226–1235
10. Mukai E, Fujimoto S, Sato H, et al. Exendin-4 suppresses SRC activation and reactive oxygen species production in diabetic Goto-Kakizaki rat islets in an Epac-dependent manner. Diabetes 2011;60:218–226
11. Kajikawa M, Fujimoto S, Tsuura Y, et al. Ouabain suppresses glucose-induced mitochondrial ATP production and insulin release by generating reactive oxygen species in pancreatic islets. Diabetes 2002;51:2522–2529
12. Nassar T, Kadery B, Lotan C, Da'as N, Kleinman Y, Haj-Yehia A. Effects of the superoxide dismutase-mimetic compound tempol on endothelial dysfunction in streptozotocin-induced diabetic rats. Eur J Pharmacol 2002;436:111–118
13. Dawson DA, Masayasu H, Graham DI, Macrae IM. The neuroprotective efficacy of ebselen (a glutathione peroxidase mimic) on brain damage induced by transient focal cerebral ischaemia in the rat. Neurosci Lett 1995;185:65–69
14. Tang C, Han P, Oprescu AI, et al. Evidence for a role of superoxide generation in glucose-induced β-cell dysfunction in vivo. Diabetes 2007;56:2722–2731
15. Wang XD, Vatamaniuk MZ, Wang SK, Roneker CA, Simmons RA, Lei XG. Molecular mechanisms for hyperinsulinaemia induced by overproduction of selenium-dependent glutathione peroxidase-1 in mice. Diabetologia 2008;51:1515–1524
16. Fujimoto S, Ishida H, Kato S, et al. The novel insulinotropic mechanism of pimobendan: direct enhancement of the exocytotic process of insulin secretory granules by increased Ca^{2+} sensitivity in β-cells. Endocrinology 1998;139:1133–1140
17. Oliveira HR, Verlengia R, Carvalho CR, Britto LR, Curi R, Carpinelli AR. Pancreatic β-cells express phagocyte-like NAD(P)H oxidase. Diabetes 2003;52:1457–1463

18. Takasu N, Yamada T, Shimizu Y. Generation of H_2O_2 is regulated by cytoplasmic free calcium in cultured porcine thyroid cells. Biochem Biophys Res Commun 1987;148:1527–1532
19. Nabe K, Fujimoto S, Shimodahira M, et al. Diphenylhydantoin suppresses glucose-induced insulin release by decreasing cytoplasmic H^+ concentration in pancreatic islets. Endocrinology 2006;147:2717–2727
20. Shimodahira M, Fujimoto S, Mukai E, et al. Rapamycin impairs metabolism-secretion coupling in rat pancreatic islets by suppressing carbohydrate metabolism. J Endocrinol 2010;204:37–46
21. Takehiro M, Fujimoto S, Shimodahira M, et al. Chronic exposure to β-hydroxybutyrate inhibits glucose-induced insulin release from pancreatic islets by decreasing NADH contents. Am J Physiol Endocrinol Metab 2005;288:E372–E380
22. Radu RG, Fujimoto S, Mukai E, et al. Tacrolimus suppresses glucose-induced insulin release from pancreatic islets by reducing glucokinase activity. Am J Physiol Endocrinol Metab 2005;288:E365–E371
23. Gardner RS. A sensitive colorimetric assay for mitochondrial alpha-glycerophosphate dehydrogenase. Anal Biochem 1974;59:272–276
24. MacDonald MJ. High content of mitochondrial glycerol-3-phosphate dehydrogenase in pancreatic islets and its inhibition by diazoxide. J Biol Chem 1981;256:8287–8290
25. Miwa I, Fukatsu H, Toyoda Y, Okuda J. Anomeric preference of glucose utilization in human erythrocytes loaded with glucokinase. Biochem Biophys Res Commun 1990;173:201–207
26. Meglasson MD, Matschinsky FM. Pancreatic islet glucose metabolism and regulation of insulin secretion. Diabetes Metab Rev 1986;2:163–214
27. Choi JH, Cho HK, Choi YH, Cheong J. Activating transcription factor 2 increases transactivation and protein stability of hypoxia-inducible factor 1α in hepatocytes. Biochem J 2009;424:285–296
28. Mysore TB, Shinkel TA, Collins J, et al. Overexpression of glutathione peroxidase with two isoforms of superoxide dismutase protects mouse islets from oxidative injury and improves islet graft function. Diabetes 2005;54:2109–2116
29. Lortz S, Tiedge M. Sequential inactivation of reactive oxygen species by combined overexpression of SOD isoforms and catalase in insulin-producing cells. Free Radic Biol Med 2003;34:683–688
30. Zhang CY, Baffy G, Perret P, et al. Uncoupling protein-2 negatively regulates insulin secretion and is a major link between obesity, β cell dysfunction, and type 2 diabetes. Cell 2001;105:745–755
31. Yoshihara E, Fujimoto S, Inagaki N, et al. Disruption of TBP-2 ameliorates insulin sensitivity and secretion without affecting obesity. Nat Commun 2010;1:127
32. Östenson CG, Abdel-Halim SM, Rasschaert J, et al. Deficient activity of FAD-linked glycerophosphate dehydrogenase in islets of GK rats. Diabetologia 1993;36:722–726
33. Malmgren S, Nicholls DG, Taneera J, et al. Tight coupling between glucose and mitochondrial metabolism in clonal β-cells is required for robust insulin secretion. J Biol Chem 2009;284:32395–32404
34. Zhao C, Rutter GA. Overexpression of lactate dehydrogenase A attenuates glucose-induced insulin secretion in stable MIN-6 β-cell lines. FEBS Lett 1998;430:213–216
35. Ainscow EK, Zhao C, Rutter GA. Acute overexpression of lactate dehydrogenase-A perturbs beta-cell mitochondrial metabolism and insulin secretion. Diabetes 2000;49:1149–1155
36. Alcazar O, Tiedge M, Lenzen S. Importance of lactate dehydrogenase for the regulation of glycolytic flux and insulin secretion in insulin-producing cells. Biochem J 2000;352:373–380
37. MacDonald MJ. Estimates of glycolysis, pyruvate (de)carboxylation, pentose phosphate pathway, and methyl succinate metabolism in incapacitated pancreatic islets. Arch Biochem Biophys 1993;305:205–214
38. Ling ZC, Efendic S, Wibom R, et al. Glucose metabolism in Goto-Kakizaki rat islets. Endocrinology 1998;139:2670–2675
39. Sekine N, Cirulli V, Regazzi R, et al. Low lactate dehydrogenase and high mitochondrial glycerol phosphate dehydrogenase in pancreatic β-cells. Potential role in nutrient sensing. J Biol Chem 1994;269:4895–4902
40. Koppenol WH, Bounds PL, Dang CV. Otto Warburg's contributions to current concepts of cancer metabolism. Nat Rev Cancer 2011;11:325–337
41. Gordan JD, Thompson CB, Simon MC. HIF and c-Myc: sibling rivals for control of cancer cell metabolism and proliferation. Cancer Cell 2007;12:108–113
42. Jaakkola P, Mole DR, Tian YM, et al. Targeting of HIF-α to the von Hippel-Lindau ubiquitylation complex by O_2-regulated prolyl hydroxylation. Science 2001;292:468–472
43. Maxwell PH, Wiesener MS, Chang GW, et al. The tumour suppressor protein VHL targets hypoxia-inducible factors for oxygen-dependent proteolysis. Nature 1999;399:271–275
44. Kim JW, Tchernyshyov I, Semenza GL, Dang CV. HIF-1-mediated expression of pyruvate dehydrogenase kinase: a metabolic switch required for cellular adaptation to hypoxia. Cell Metab 2006;3:177–185
45. Cantley J, Selman C, Shukla D, et al. Deletion of the von Hippel-Lindau gene in pancreatic β cells impairs glucose homeostasis in mice. J Clin Invest 2009;119:125–135
46. Puri S, Cano DA, Hebrok M. A role for von Hippel-Lindau protein in pancreatic β-cell function. Diabetes 2009;58:433–441
47. Gerald D, Berra E, Frapart YM, et al. JunD reduces tumor angiogenesis by protecting cells from oxidative stress. Cell 2004;118:781–794
48. Kaelin WG Jr, Ratcliffe PJ. Oxygen sensing by metazoans: the central role of the HIF hydroxylase pathway. Mol Cell 2008;30:393–402